CHAPTER 4

MAPPING NEMATODE DIVERSITY IN THE SOUTHERN BIGHT OF THE NORTH SEA

Adapted from: Merckx, B., Van Meirvenne, M., Steyaert, M., Vanreusel, A., Vincx, M., Vanaverbeke, J., 2010. Mapping nematode diversity in the Southern Bight of the North Sea. Marine Ecology Progress Series 406, 135-145.

CHAPTER 4

MAPPING NEMATODE DIVERSITY IN THE SOUTHERN BIGHT OF THE NORTH SEA

ABSTRACT

In order to protect the biodiversity of the seas from, e.g. overexploitation, the spatial distribution of biodiversity and the mapping of biodiversity hotspots are of great importance. In the present paper we discuss different methods to develop full coverage biodiversity maps of free-living marine nematodes in the Southern Bight of the North Sea. A database with sampling data, gathered over 3 decades (1972 to 2004), combined with exhaustive environmental data, was employed to predict species richness and the expected number of species by different methods: ordinary kriging (OK) and regression kriging (RK) with ordinary least squares (OLS) and generalised least squares (GLS). The predictive value of these methods was evaluated by an independent validation set. Replicate samples were used to make an accurate estimation of the nugget variance, since replicates reveal local variability. Accordingly, it was feasible to find a spatial pattern in the residuals of the regression models. Our analysis pointed out that GLS improved the OK models substantially, while RK only slightly improved the GLS model. The diversity of marine nematodes is substantially influenced by the silt-clay fraction and the amount of total suspended matter, which is also reflected in the resulting map with a species-poor area near the coast line, especially near the south of the mouth of the Scheldt estuary. Off coast diversity and evenness are generally higher.

Key words

Nematoda, diversity, geostatistics, North Sea, mapping, generalised least squares

INTRODUCTION

The ocean floor is a heterogeneous environment with marine biota patchily distributed. Therefore, diversity and densities of marine communities tend to be higher in localised areas (Reese and Brodeur, 2006). Moreover, the marine seabed is increasingly disturbed and degraded by bottom trawling, sand extraction, dredging and dumping, which inevitably reduces biological diversity. Identification of diversity hotspots is a major concern in diversity conservation, and the identification of these marine, biological hotspots is a growing area of research (Malakoff, 2004; Reese and Brodeur, 2006). Biodiversity indices are often used to describe these areas of biological interest. However, studies investigating diversity in large areas are scarce, due to the high costs involved in such a labour-intensive process, and most studies result in point observations, while there is a growing need for full coverage maps.

Geostatistical interpolation techniques offer a powerful and cost-effective alternative; based on available point observations of communities and full coverage maps of relevant environmental data, full coverage maps of diversity can be constructed. Kriging has been developed for spatially structured mining data (Matheron, 1963) and is widely used in the terrestrial environment to create maps of chemical properties of soil and air (Hengl *et al.*, 2004; Hoek *et al.*, 2008; Van Meirvenne *et al.*, 2008) and more recently it has been applied to model faunal (Walker *et al.*, 2008) and floral (Hernández-Stefanoni and Dupuy, 2007) distributions. In the marine environment, it has been employed to map soil characteristics (Verfaillie *et al.*, 2006), distribution patterns of marine species (Mello and Rose, 2005; Rios-Lara *et al.*, 2007) and, to a lesser extent, diversity (Reese and Brodeur, 2006). In the present study, 2 conceptually different approaches were used: (1) interpolation relying only on point observations of the diversity index, known as ordinary kriging (OK) and (2) interpolation based on both point observations and full coverage environmental maps, known as regression kriging (RK).

In the present study, we focused on free-living marine benthic nematodes, a taxon within the meiofauna, comprising metazoans passing through a 1 mm mesh sieve but retained on a 38 µm mesh sieve. To our knowledge, these geostatistical techniques have not been applied before on Nematoda. This is surprising since these free-living roundworms represent the highest metazoan diversity in many benthic environments in terms of species numbers (Heip *et al.*, 1985): >50 species are commonly found in a single 10 cm^2 core. Owing to their interstitial lifestyle, properties of the sediment, such as grain size distribution, the silt-clay fraction and food availability, have a strong influence on the diversity and composition of nematode assemblages (Heip *et al.*, 1985; Vanreusel, 1990; Vincx, 1990; Steyaert *et al.*, 1999). Nematode communities seem to be resilient to disturbance, and their restoration occurs easily after temporal, low impacts (Kennedy and Jacoby, 1999; Schratzberger *et al.*, 2002), making them a perfect community to model based on long-term environmental and full coverage data. Previous research on the predictability of nematode diversity did indeed

yield accurate predictive models (Merckx *et al.*, 2009); yet, these were not area-covering models.

The research area is the Southern Bight of the North Sea. The seafloor is not at all homogeneous as it is characterised by sand dunes and a wide range of sediment types, varying from muddy to sandy environments (Lanckneus *et al.*, 2002). The coastal area is characterised by a high amount of total suspended matter, chlorophyll *a* (chl *a*) and silt-clay fraction, especially near the Belgian coast. The primary objective of the present study was to create accurate biodiversity maps of the nematode diversity of the Southern Bight of the North Sea.

MATERIALS AND METHODS

Study area

The research area, with a total surface of about 18 000 km^2, is situated in the Southern Bight of the North Sea, near the Belgian and the Dutch coastal area (latitude: 51°6'2'' to 52°59'19'' N; longitude: 2°14'39'' to 4°30'43'' E).

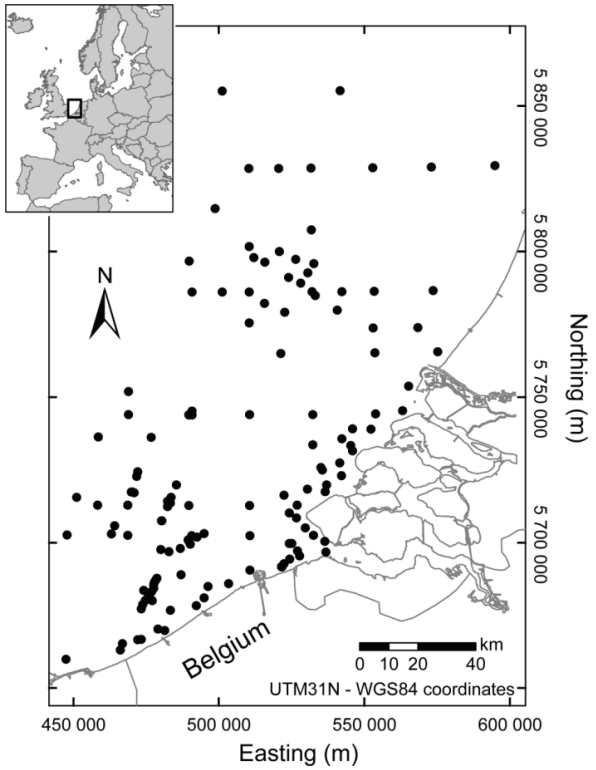

Fig. 4.1. Study area and location of the sampling stations (•).

Nematode data

The nematode data were retrieved from the MANUELA database. Within the EU Network of Excellence MarBEF, MANUELA is a Research Project focusing on meiobenthic assemblages. The MANUELA database was compiled capturing the available data on meiobenthos on a

broad European scale (Vandepitte *et al.*, 2009). For the present paper, the area of research was restricted to the Southern Bight of the North Sea, since, firstly, full coverage environmental maps were available for the entire region and, secondly, results were not biased by sampling strategy because all data were collected by a single institute, the Marine Biology Research Group of Ghent University. The resulting dataset consisted of 562 samples belonging to 153 different stations (Fig. 4.1). These data included information on 99 966 nematodes identified to species level and collected in the time frame from 1972 to 2004. Different sampling gears were used to collect these data: 49% of the samples were taken with a Reineck box corer, 31% with a Van Veen grab, 19% with a NIOZ box corer and 1% by divers. All subsamples were taken with Perspex cores, with a surface area of 10 cm^2.

Environmental data

The source of the environmental data can be divided into 2 groups: from maps acquired by remote sensing and from maps derived from data sampled in the field.

The first group of data was derived from remote sensing by the MERIS spectrometer on board the Envisat satellite of the ESA and comprises data on total suspended matter and chl *a* in the water column (Park *et al.*, 2006). For the time frame from 2003 to 2005, 80 maps of chl *a* and 90 maps of total suspended matter were available. These maps were reduced to 3 maps for each variable, containing biologically relevant information: the minimum, maximum and average values. This data reduction technique is often applied in ecological modelling (Loiselle *et al.*, 2008; Cunningham *et al.*, 2009; Echarri *et al.*, 2009). Through sedimentation and degradation, chl *a* and total suspended matter enrich the bottom organic matter (Druon *et al.*, 2004). This input of organic matter is known to influence nematodes directly, as it serves as a food source (Vanaverbeke *et al.*, 2004b; Franco *et al.*, 2008), or indirectly, as microbial degradation often results in oxygen-stressed sediments (Graf, 1992), which can have a strong adverse effect on nematode diversity (Steyaert *et al.*, 1999).

The second group comprised data on sediment characteristics and bathymetry. The sediment was described by the median grain size and the silt-clay fraction. These maps were supplied by the Renard Centre of Marine Geology, Ghent University (Verfaillie *et al.*, 2006), and by the TNO Built Environment and Geosciences 'Geological Survey of the Netherlands'. The bathymetrical data were provided by the Ministry of the Flemish Community Department of Environment and Infrastructure, Waterways and Marine Affairs Administration, Division Coast, Hydrographic Office and completed with data from the Hydrographic Service of the Royal Netherlands Navy and by the Directorate-General of Public Works and Water Management of the Dutch Ministry of Transport, Public Works and Water Management. The silt-clay fraction and the median grain size are important factors determining meiobenthic diversity (Heip *et al.*, 1985; Steyaert *et al.*, 1999; Vanaverbeke *et al.*, 2002; Merckx *et al.*, 2009). Depth in shallow waters does not directly affect the nematode community, but it modifies the effects of other factors, such as trophic conditions, sediment properties and current properties.

An overview of the range of the environmental data in the dataset is shown in Table 4.1. The range is calculated for both the database, used to build the model, and for the full coverage maps, used for model application.

		Database			Maps		
Parameter	Description	Min.	Max.	Median	Min.	Max.	Median
S	species richness	1	77	30			
ES(25)	expected species richness	1	19	13			
d50	median grain size (µm)	99	541	261	4	692	317
Silt-clay	silt-clay fraction (%)	0.01	95	1.3	0	84	0.053
TSM_mean	average total suspended matter ($g.m^{-3}$)	1.9	24	8.1	1	24	2.6
TSM_max	maximum total suspended matter ($g.m^{-3}$)	3.8	50	28	2.3	66	7.3
TSM_min	minimum total suspended matter ($g.m^{-3}$)	0.55	10	1.2	0.2	14	0.8
Chl_mean	average chlorophyll *a* ($mg.m^{-3}$)	2	12	4.9	1.3	26	3.2
Chl_max	maximum chlorophyll *a* ($mg.m^{-3}$)	4.3	35	22	2.7	39	12
Chl_min	minimum chlorophyll *a* ($mg.m^{-3}$)	0.04	2.3	1.3	0.04	20	1.1
Depth	depth of the water column (m)	2	44	15	-1.3	53	26
Year	year of sampling	1971	2004	1985			

Table 4.1. Range and median values of diversity indices (first 2 parameters) and environmental variables of the dataset used to build the models (database), and of the environmental variables in the maps (maps)

Diversity indices

As nematodes can occur in large numbers, nematode identification is generally carried out on a subsample. Subsamples consist mostly of 200 individuals, although the exact number of identified nematodes varies between samples. Therefore, we used a diversity measure that is independent of sampling effort: the expected number of species. The ES(*n*) is the expected number of species if the sample were of the smaller size n (Hurlbert, 1971). When individuals are independently sampled with similar probability from a small sample, the expected species richness is (Sanders, 1968; Hurlbert, 1971; Simberloff, 1972):

$$\mathrm{ES(n)} = \sum_{i=1}^{S}\left[1 - \frac{\binom{N-x_i}{n}}{\binom{N}{n}}\right] \qquad \text{(Eq. 4.1)}$$

where N is the total number of individuals in the sample, S is the total number of species (i.e. species richness), x_i is the number of individuals of species i in the sample and n is the number of individuals in the subsample. The term inside the summation sign is the probability that a sample of n individuals will contain species i (Gotelli and Graves, 1996). Previous research on the predictability of nematode diversity showed that models developed for ES(25) yielded good predictions (Merckx *et al.*, 2009).

The species richness (S), although not independent of sampling effort, was included in the analysis as well, since it is the most commonly used index and is representative for most of

the samples because the sampling methodology remained unchanged over the years. The range of diversity indices in the dataset is shown in Table 4.1.

Geostatistical modelling

Geostatistics offers powerful interpolation methods for spatial analyses, especially in a patchy environment. The cornerstone in geostatistics is the modelling of the variogram (Webster and Oliver, 2007). It represents the average variance between observations separated by a distance $\boldsymbol{h}$ and has a strong descriptive and interpretative power for the structure of the spatial variability of a variable. The variogram is estimated by (Journel and Huijbregts, 1978; Goovaerts, 1997):

$$\gamma(\boldsymbol{h}) = \frac{1}{2N(\boldsymbol{h})} \sum_{\alpha=1}^{N(\boldsymbol{h})} \{z(\boldsymbol{x}_\alpha + \boldsymbol{h}) - z(\boldsymbol{x}_\alpha)\}^2 \qquad \text{(Eq. 4.2)}$$

with $\gamma(\boldsymbol{h})$ being the variogram for a distance vector (lag) $\boldsymbol{h}$ between observations $z(\boldsymbol{x}_\alpha)$ and $z(\boldsymbol{x}_\alpha + \boldsymbol{h})$ of the diversity at the locations $\boldsymbol{x}_\alpha$ and $\boldsymbol{x}_\alpha + \boldsymbol{h}$ and with $N(\boldsymbol{h})$ being the number of pairs separated by $\boldsymbol{h}$.

A variogram is represented as a graph and reveals the underlying spatial pattern of variables, having more similar values when they are spatially closer. The experimental variogram is a plot of the calculated $\gamma(\boldsymbol{h})$ values versus the lag $\boldsymbol{h}$, while the theoretical variogram is the curve fitted through these points, yielding a continuous function of $\gamma(\boldsymbol{h})$ (Fig. 4.2). This curve fitting procedure is a crucial step in variogram analysis (Webster and Oliver, 2007). Four important variogram characteristics can be derived: the sill, the range, the nugget and the model type. The 'sill' represents the total variance of the variable and is the maximum of the variogram model. The 'range' is the maximal spatial extent of spatial correlation between

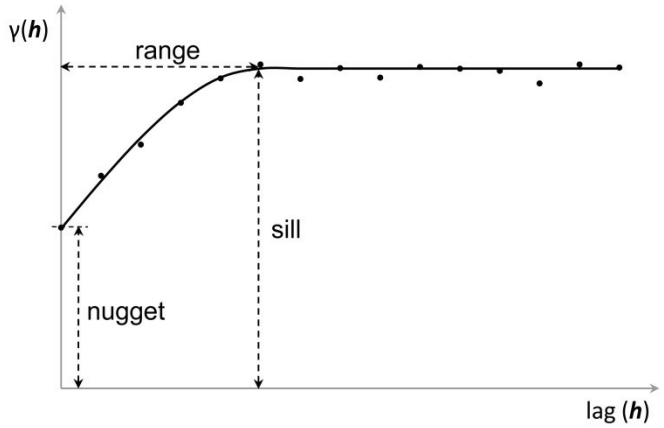

Fig. 4.2. Experimental variogram (dots) and the fitted theoretical variogram (line). The latter is a function describing the degree of spatial dependence of a spatial variable. The plot shows the relation between the semivariance $\gamma(\boldsymbol{h})$ of the variable and the distance $\boldsymbol{h}$ between paired data. The nugget (or nugget variance) is the variance at the limit as the lag tends to zero; the sill is the limit of the variogram at infinite lag distances and the range is the distance at which the difference between the variogram and the sill becomes negligible.

observations of the variable. At lags larger than the range, the expected difference between observations is maximal (being the sill) and independent of the distance. The extrapolation of the variogram model to lags of 0 is called the 'nugget variance' and represents sources of random noise, such as sampling errors and variability at distances closer than the smallest sampling lag. The relative structural variance, i.e. the proportion of total variance that can be attributed to the spatial autocorrelation, can be derived from the variogram: it is the total variance minus the nugget, divided by the total variance. The theoretical variogram can be composed of nested models or structures. Common models are the spherical, exponential, Gaussian and power model. If the variable shows anisotropic variability, directional variograms can be derived (Journel and Huijbregts, 1978; Verfaillie *et al.*, 2006). All variograms were calculated and constructed with the software Variowin 2.2 (Panatier, 1996).

In biological applications it is common to collect replicate samples at nearly the same sampling point to check for local variation in species communities. These replicates have the same geographical coordinates, but are in reality some metres apart, since they result from different drops. Due to limitations of the software, it is impossible to use these replicates in variogram modelling since they have the same coordinates. However, by randomly adding a realistically small variation, within a range of metres, these replicates can be used to accurately estimate the nugget effect.

Two geostatistical interpolation techniques were used in the present paper: OK and RK. OK does not need auxiliary information. However, when such information is available and it is related to the variable of interest, RK often outperforms OK because it exploits this additional information (Hengl *et al.*, 2007).

The OK algorithm uses a weighted linear combination of sampled points situated around the location $\boldsymbol{x_0}$, where the interpolation is conducted. Observations closer to $\boldsymbol{x_0}$ get a higher weight than observations further away. An underlying assumption for OK is that the mean value is locally stationary; thus, it has a constant value inside the interpolation window. The algorithm can be written as:

$$Z^*_{OK}(\boldsymbol{x}_0) = \sum_{\alpha=1}^{n(\boldsymbol{x_0})} \lambda_\alpha \, Z(\boldsymbol{x}_\alpha) \qquad \text{(Eq. 4.3)}$$

with $n(\boldsymbol{x_0})$ being the total number of observations in the interpolation window around $\boldsymbol{x}_0$ and λ_α being the weight attributed to the observation $Z(\boldsymbol{x}_\alpha)$. The weights λ_α are obtained by solving a set of equations involving knowledge of the variogram, and they are chosen in such a way that the prediction error variance is minimised (Webster and Oliver, 2007).

When exhaustive secondary information is available, RK can be used alternatively. Predictions by RK involve 2 steps: first, the relationship between the primary variable and the secondary environmental variables at the sampling locations are modelled by a linear regression, and this model is then applied to the unsampled locations using the environmental variables at this location. Second, the residuals of this linear model are subjected to simple kriging (SK) with an expected mean of 0 (Deutsch and Journel, 1992).

The linear model can be written as a linear combination of the environmental variables:

$\hat{Z}(\boldsymbol{x}_0) = \sum_{k=0}^{p} \hat{\beta}_k \, q_k(\boldsymbol{x}_0) \qquad q_0(\boldsymbol{x}_0) \equiv 1$ (Eq. 4.4)

where $q_k(\boldsymbol{x}_0)$ is the value of the independent variable k at the location $\boldsymbol{x}_0$, $\hat{\beta}_k$ is the estimated regression coefficient of the variable k and p is the number of dependent variables. In the current study, the regression coefficients are estimated in 2 ways: by ordinary least squares (OLS) and generalised least squares (GLS). The latter is an iterative technique (Carroll and Rupert, 1988), which takes the spatial correlation between observations into account (Cressie, 1993). Different steps were carried out for both linear regression techniques. First, variables where standardised to a mean of 0 and a standard deviation of 1, to understand the relative importance of each environmental variable (Schroeder *et al.*, 1986). Secondly, multicollinear variables with a Pearson product-moment correlation coefficient of >0.8 were removed, and, ultimately, by backwards selection, only the highly significant terms were retained from a second-order full model. Normality of the residuals was checked at a significance level of $p < 0.05$. In case no normality was found, the primary variable was log-transformed.

As mentioned before, RK combines 2 approaches: linear regression (the first term in Eq. 4.5) and simple kriging with an expected mean of 0 for the residuals of the linear model (the second term in Eq. 4.5). Thus, the complete model can be written as (Hengl *et al.*, 2007):

$\hat{Z}(\boldsymbol{x}_0) = \sum_{k=0}^{p} \hat{\beta}_k \, q_k(x_0) + \sum_{\alpha=1}^{n(x_0)} \lambda_\alpha \, e(\boldsymbol{x}_\alpha) \qquad q_0(\boldsymbol{x}_0) \equiv 1$ (Eq. 4.5)

where $e(\boldsymbol{x}_\alpha)$ is the residual at location $\boldsymbol{x}_\alpha$.

Validation

A quality control of the different models was performed using a validation dataset containing 30% of all the samples, leaving 70% of the data for the training set. Samples were randomly assigned to the validation set; however, replicates were kept in the same dataset. Replicate samples are, due to spatial autocorrelation, more alike than other samples. If replicate samples are distributed over both sets, the values of the validation set will be predicted accurately, since similar values are present in the training set. This will result in overly optimistic model statistics. As a consequence, keeping replicates in the same dataset will give a more realistic estimation of the accuracy of the geographic interpolation. This validation dataset was used exclusively at the completion of the analysis to compare the performance of the different modelling techniques. Therefore, 5 statistics were calculated: the mean estimation error (MEE) (Eq. 4.6), the root mean-square estimation error (RMSEE) (Eq. 4.7), the mean absolute estimation error (MAEE) (Eq. 4.8), the Pearson product-moment correlation coefficient and the Spearman rank correlation coefficient.

$MEE = \frac{1}{n} \sum_{\alpha=1}^{m} \left(z^*(\boldsymbol{x}_\alpha) - z(\boldsymbol{x}_\alpha) \right)$ (Eq. 4.6)

$RMSEE = \sqrt{\frac{1}{n} \sum_{\alpha=1}^{m} \left(z^*(\boldsymbol{x}_\alpha) - z(\boldsymbol{x}_\alpha) \right)^2}$ (Eq. 4.7)

$MAEE = \frac{1}{n} \sum_{\alpha=1}^{m} |z^*(\boldsymbol{x}_\alpha) - z(\boldsymbol{x}_\alpha)|$ (Eq. 4.8)

where m is the number of validation points, $z(\boldsymbol{x}_\alpha)$ is the measurement and $z^*(\boldsymbol{x}_\alpha)$ is the estimation at the same location. The MEE determines the degree of bias in the estimates; the RMSEE, like the MAEE, evaluates the magnitude of the average error; however, the latter is less sensitive to outliers. The Pearson product-moment correlation coefficient indicates the strength of the linear relationship between the predicted and the observed values of the validation set, and the Spearman rank correlation coefficient is the non-parametric estimation of the correlation between the observed and predicted values. Another way to analyse the validation error is by applying Chebyshev's inequality theorem. According to his theorem the proportion of normalised errors should be ≤1/9 (Hengl, 2007).

Practically, 5 different models were compared with this validation set: the model obtained by OK, the linear models determined by OLS and GLS without kriging (the first term in Eq. 4.5), and both linear models combined with kriging (both terms in Eq. 4.5). Based on the results of this validation set, the models with the best values for the test statistics were selected, and the whole dataset was used to create the final maps.

RESULTS

Linear regression with OLS and GLS

For each diversity index, 2 linear models are constructed (Table 4.2). After selecting the most significant variables, the final models include only 2 or 3 variables, namely the silt-clay fraction, minimum values of total suspended matter and the year of sampling. It is clear from Table 4.2 that the silt-clay fraction has the strongest explanatory power of all models. At least 10 observations are recommended per predictor to prevent overfitting (Hengl *et al.*, 2007). This condition is clearly met: in the training set there are 406 observations and 5 predictor variables. The coefficients of the 2 regression techniques are similar, indicating that no strong spatial clustering is present between the points (Hengl *et al.*, 2004).

Model		Intercept	Silt-clay	(Silt-clay)²	TSM_min	Year	R²
Log(S)	OLS	2.76	-0.81	0.34	-0.33	0.15	0.68
	GLS	2.75	-0.87	0.33	-0.28	0.1	0.66
ES(25)	OLS	9.53	-5.36	1.73	-1.57		0.73
	GLS	9.49	-5.33	1.59	-1.36		0.73

Table 4.2. Estimates of the regression coefficients of the linear models and coefficient of determination (R^2) of the models. The logarithm of the species richness, log(S), and the expected species richness, ES(25), were modelled by ordinary least squares (OLS) and generalised least squares (GLS). See Table 4.1 for definitions of parameters.

Variogram analysis

For each diversity index 3 variograms are modelled: 1 used for OK and 2 for RK. The latter 2 are inferred from the residuals of both linear regression techniques, OLS and GLS (Fig. 4.3). Directional variograms that were apparent in earlier research on the Belgian Continental Shelf (Verfaillie *et al.*, 2006) do not improve model performance and are omitted from the results. The variograms for OK reveal a strong spatial structure for both diversity indices, with a range of >40 km and a relative structural variance of almost 90%, which indicates that a large fraction of the total variance can be linked to spatial processes (Table 4.3). For this database, replicate samples were taken within ranges of metres, while the total area has a maximum cross section of 250 km; thus, the variation between replicate samples is at the same time an accurate estimate of the nugget. The variograms used for RK and inferred from the residuals of the linear regression models show a significant decrease in range and sill for both diversity indices. This reflects the effect of the linear regression: a considerable amount of variation in the data is explained by the linear regression, and the extent of the spatial dependency of the residuals is much smaller than that of the original diversity index. For instance, the initial relative structural variance is about 90% for both parameters and decreases to about 65-69% with GLS. The range decreases by 84% for ES(25) and with >90% for S.

For ES(25) both modelling techniques result in the same decrease of the relative structural variance. For the species richness, however, there is a marked difference between GLS and OLS: GLS is able to explain more of the relative structural variance than OLS, indicating a better performance of this modelling technique.

			Nugget	Range (km)	Sill	Relative structural variance (%)	Model
S	OK	S	44	42.7	320	88	spherical
	RK	residuals OLS	37	3.2	90	71	spherical
	RK	residuals GLS	34	2.6	76	69	spherical
ES(25)	OK	ES(25)	4.3	47.5	36.5	89	spherical
	RK	residuals OLS	3.1	13.6	5.8	65	spherical
	RK	residuals GLS	3	10.9	5.6	65	spherical

Table 4.3. Variogram parameters (see Fig. 4.3 for description). OK: ordinary kriging; RK: regression kriging; OLS: ordinary least squares; GLS: generalised least squares.

Independent validation

The independent validation set enables us to compare the efficiency of the different modelling techniques. Both regression techniques improve the model for ES(25) and S considerably compared to OK (Table 4.4). Therefore, the relation between the diversity and the environmental variables exists and explains a considerable amount of the variation in diversity. Nevertheless, there is still some spatial pattern present in the residuals; hence,

other unknown or fine-scaled factors may contribute to the geographical distribution of nematode diversity.

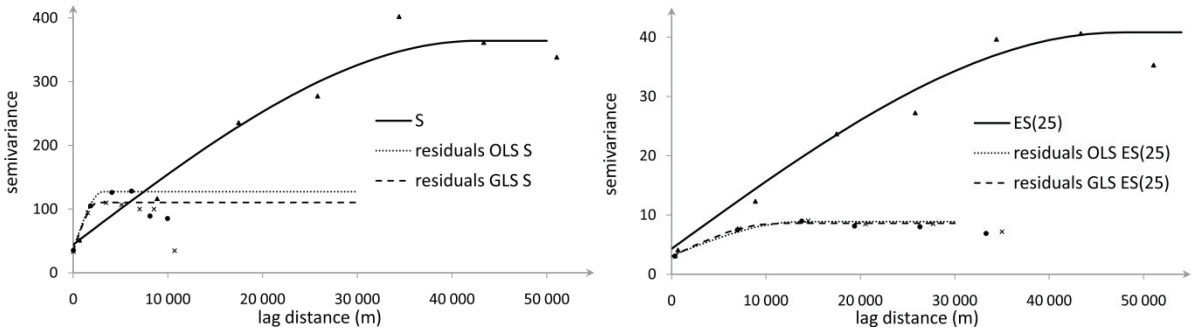

Fig. 4.3. Theoretical variograms of S (left) and ES(25) (right) (see Table 4.1) fitted to the experimental values of the diversity index and used for ordinary kriging (▲), to the residuals of the ordinary least squares (OLS) model (●), and to the residuals of the generalised least squares (GLS) model (×). The latter 2 are used for regression kriging.

Comparison of both regression techniques for both diversity indices shows that GLS offers the best models, kriging with GLS enhances some, but not all, of the model performance indices. The major improvement is found for the MEE; thus, kriging can account for the remaining bias of the linear models. For species richness, there is a clear difference between the Pearson product-moment correlation and Spearman rank correlation coefficients, indicating that there are some strong outliers present in the residuals. This is less pronounced for ES(25). Overall, higher correlation values were found for ES(25). All models meet Chebyshev's inequality condition, implying that there are not an unusually high number of locations where the errors are much higher than at other stations.

Biodiversity index	Linear model	Kriging technique	MEE	RMSE	MAEE	Pearson	Spearman
S	No model	OK	0.39	14.99	11.35	0.37	0.83
	OLS	No kriging	1.17	12.41	10.08	0.61	0.85
	OLS	RK	0.56	12.35	9.86	0.60	0.85
	GLS	No kriging	-0.53	**11.76**	9.46	**0.63**	0.86
	GLS	RK	**-0.37**	11.84	**9.42**	0.62	**0.87**
ES(25)	No model	OK	**0.02**	3.63	2.52	0.57	0.87
	OLS	No kriging	-0.26	2.67	2.14	0.80	0.84
	OLS	RK	0.04	2.56	2.04	0.80	0.87
	GLS	No kriging	-0.51	2.65	2.14	**0.81**	0.85
	GLS	RK	-0.06	**2.55**	**2.03**	0.80	**0.88**

Table 4.4. Statistics of predicted and observed values of the independent validation set. Best values for each diversity index are in bold. MEE: mean estimation error; RMSEE: root mean-square estimation error; MAEE: mean absolute estimation error; OK: ordinary kriging; RK: regression kriging. See Table 4.1 for further definitions.

Final maps

Final maps were constructed with all the available data (Fig. 4.4), resulting in 2 similar charts: near the Belgian coast there is a very low diversity. On average, only 9 species per sample were found in this region and ES(25) is about 4.4, while, for the whole region, an average number of 30 species per sample were found, yielding an average ES(25) of 11.8. Further offshore, the diversity increases considerably. Within this diverse area, there are small patches with high and low diversity, resulting from individual sampling points with higher or lower diversity than the surrounding samples. The range of these patches is larger for ES(25), since the range of the spatial dependency of the residuals is larger for this index.

DISCUSSION

Linear regression

The final linear regression functions all comprise a linear and quadratic function of the silt-clay fraction, which results in a positive parabola with a minimum diversity situated around 60% silt-clay. Consequently, the influence of silt-clay is not unequivocal; when the silt-clay fraction exceeds this threshold, the influence becomes less detrimental. This is contradictory to the general belief that the silt-clay fraction has a purely adverse effect on nematode diversity (Heip *et al.*, 1985; Vanreusel, 1990; Vanaverbeke *et al.*, 2002). However, in the case of strongly oxidised sediments, a positive relation between the silt-clay fraction and nematode diversity has been reported before (Steyaert *et al.*, 1999). A full coverage map of the redox potential was not available; however, organically enriched benthic environments are often encountered in areas with a high load of total suspended matter (TSM). High TSM values result in a reduced environment, and low values may permit highly oxidised sediments. Consequently, the negative correlation of species diversity with TSM may account for this effect.

The linear models indicate that in recent years the observed species richness (S) has increased. But this ‘effect’ is observed because in the last decade only environments with <20% silt-clay, thus with high species richness, were sampled. However, the relationship between the year of sampling and ES(25) is not significant. Similarly to S, low values of ES(25) were not found during the last decade, but the maximum values stayed almost the same over the whole period, remaining at a value of 20. This is due to the fact that ES(25) is a standardisation technique and is bound to an upper limit of 25.

Both diversity indices represent different aspects of the nematode assemblages: ES(25) is strongly influenced by the evenness of the nematode assemblage and to a lesser extent by species richness. Earlier research (Merckx *et al.*, 2009) already pointed out that evenness results in the best predictive models. Moreover, ES(25) is not dependent on sampling effort if sample area (cross-section) is the same for all samples and can therefore more readily be applied to heterogeneous data, originating from different sources.

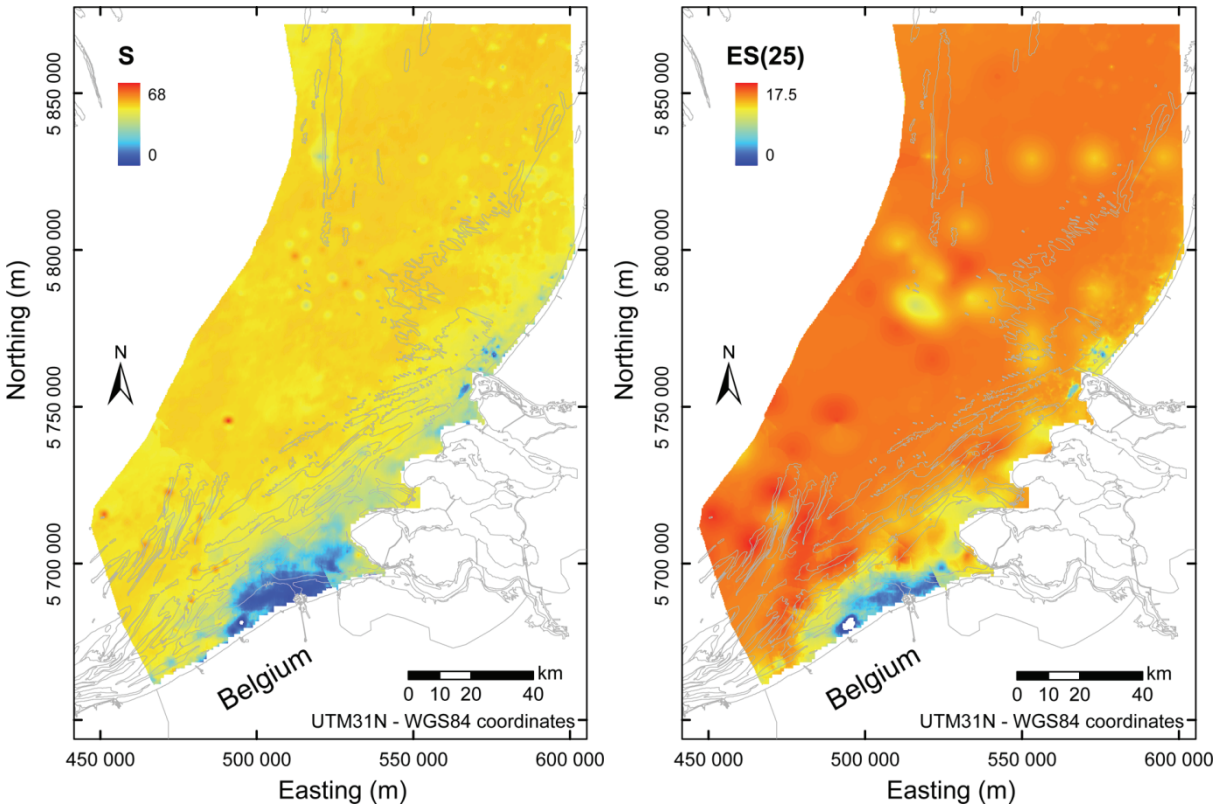

Fig. 4.4. Maps of the generalised least squares models, predicting the nematode diversity after kriging of diversity indices S (left) and ES(25) (right). Grey lines in water are bathymetric lines.

Model comparison

According to the results of the independent validation set (Table 4.4), RK performs better than OK in all cases. Therefore, the environmental variables explain a substantial part of the variation in the diversity of the nematode assemblage. The different variogram parameters underpin this result: the sill and range are much smaller for the variograms of the residuals.

The nugget is accurately estimated by including the sample replicates in the analysis. Since the purpose of replicates is indeed to assess the variance between samples, it is, at the same time, an excellent estimate for the local variation between samples. Instead of lumping or averaging these data, it is useful to keep them apart. In this way there are 2 913 station pairs within the smallest range found (2.6 km for the residuals of GLS of S), rather than only 23 pairs within this lag class, if replicates were to be averaged, which is less than the recommended 30 to 50 pairs (Journel and Huijbregts, 1978). In this case, the remaining spatial pattern in the residuals of the species richness would remain undetected and only a nugget effect would have been observed. As a consequence, the best model would have been the linear model without kriging.

Comparing both regression methods points out that, especially for S, GLS outperforms OLS. This is not surprising, since the iterative process of GLS minimises spatial autocorrelation and estimates the regression coefficients more accurately. However, according to Kitanidis

(1993), OLS may often be satisfactory because the iterative process of GLS, after an initial OLS, results in a negligible difference in the regression parameters, which was the case for ES(25) in our research.

Kriging improves, although to a lesser extent, the linear regression models. For data which are unevenly distributed, e.g. the samples on Kwintebank (51°15' N, 2°40' E), kriging has a declustering effect, because it takes both the distance to the interpolation point and the sampling configuration into account. Therefore, it is preferable to non-declustering techniques, such as linear regression (Verfaillie *et al.*, 2006).

Final maps

The resulting maps of species richness S and expected species richness ES(25) look quite similar, although both indices represent different aspects of diversity; S gives an indication of the number of species that are expected to be found in a 10 cm^2 sample in a certain area, while ES(25) expresses both species richness and evenness. Thus, it seems that, in nematode samples in the North Sea, both species richness and evenness increase in offshore regions. This is in strong contrast with the coastal region. Especially the region south of the Scheldt estuary has a very low diversity. This area is characterised by sediments with a high amount of silt-clay and a water column with elevated concentrations of chl *a* and TSM. Low nematode diversity in oxygen-stressed, fine sediments has been described before (Vincx, 1990; Steyaert *et al.*, 1999), but a link, although indirect, between nematode diversity and water column characteristics has never been shown before. Indeed, oxygen stress in marine sediments is caused by the microbial mineralisation of water column-derived organic matter (Graf, 1992), and our model indicates the link between water column processes and benthic diversity patterns.

Limitations to this research

Hengl *et al.* (2007) pointed out some limitations to RK concerning data quality, undersampling and extrapolation. Our data are historical data, supplied by different researchers within the Marine Biology Section of Ghent University. This has the advantage that sampling and identification techniques are similar. However, different types of sampling effort (e.g. small subsamples or complete cores identified) may have been applied depending on the intention of the original research. These differences can influence S, but will only slightly affect ES(25).

The predictive maps are created for a large area and are based on the data from 153 different stations and 562 samples. Variograms are typically derived from 100 to 200 observations, and, the larger the number of stations, the more precise the estimation is (Webster and Oliver, 2007). The results of the validation set indicate that kriging only slightly improves the model, which is probably due to the large average distance between the sampling points. The distance between the sampling points is often larger than the range of spatial autocorrelation of the residuals, so kriging will not alter the values of these points.

Including new data points will result in intersecting ranges for the residuals as well, and kriging will then result in better estimates.

Extrapolation of the model outside the feature area can be interpreted in 2 ways: extrapolation outside the geographical area and extrapolation for unknown environments. Concerning the geographical extrapolation, special caution should be taken when deriving data near the border of an area or in regions where few samples were taken. Regarding the environmental extrapolation, clearly the model is only suitable for known environments. Particularly for this research, all samples were taken with cores in soft sediments. Consequently, in environments where this sampling technique is not applicable, no data are available; therefore, the model is only valid for well-known sandy environments and cannot extrapolate for, e.g., hard substrates. It is clear from Table 4.1 that the data in the dataset cover nearly the complete range in the maps of the environmental variables. Only the most extreme values are not represented in the dataset. For these data, as well as unrepresented combinations of the environmental data, the model should be interpreted with caution.

Another potential issue is the limited variation in the environmental variables for the offshore region and the large distance between the sampling points. Since no environmental parameter could be identified that explains the differences in diversity in this region, the best model is the average value of the diversity indices for this area.

The kriging algorithm is based on the assumption that the measurements at a certain point are error-free, which is usually acceptable given the much larger spatial variability. The station values obtained by the GLS regression are corrected by the kriging algorithm with the *in situ* measured values. Consequently, the stations appear to be spots on the map. To optimise these maps, more relevant environmental variables and more sampling points would be needed in this area.

CONCLUSIONS

The growing need for detailed maps of biodiversity hotspots can be successfully fulfilled by regression and interpolation techniques, such as GLS and RK. When data are assembled from different sources, it is advisable to use diversity indices that are not dependent on sampling effort. In our case, ES(25) resulted in the best models: highest correlations and no outliers. The diversity of marine nematodes is substantially influenced by silt-clay and TSM, which is also reflected in the resulting map with a species-poor area near the Belgian coast.

ACKNOWLEDGEMENTS

This research is funded by the Fund for Scientific Research (FWO) of the Flemish government (FWO07/ASP/174). The authors thank all the data providers! The environmental data were gathered from different institutes: the ESA and MUMM/RBINS are acknowledged for providing and processing MERIS data (chlorophyll and TSM data, www.mumm.ac.be/BELCOLOUR); the Renard Centre of Marine Geology (RCMG,

www.rcmg.ugent.be) of Ghent University and the Hydrographic Service of the Royal Netherlands Navy and the Directorate-General of Public Works and Water Management of the Dutch Ministry of Transport, Public Works and Water Management, for the oceanographic and sedimentological data. Special thanks to the Flanders Marine Institute (VLIZ, www.vliz.be) for help in building the biological database. This research was conducted within the MANUELA framework (www.marbef.org/projects/Manuela), which is a Responsive Mode Project undertaken as part of the MarBEF EU Network of Excellence 'Marine Biodiversity and Ecosystem Functioning', which is funded by the Sustainable Development, Global Change and Ecosystems Programme of the European Community's Sixth Framework Programme (Contract No. GOCE-CT-2003-505446). This publication is Contribution Number MPS-09033 of MarBEF. This research was also supported by the GENT-BOF Project 01GZ0705 Biodiversity and Biogeography of the Sea (BBSea). We also thank the reviewers for their in-depth questions and helpful suggestions to improve the quality of this manuscript.